Environmental Science & Technology

pubs.acs.org/est

Article

Formation and Transport of Secondary Contaminants Associated with Germicidal Ultraviolet Light Systems in an Occupied Classroom

Seongjun Park, Youngbo Won, and Donghyun Rim*

Cite This: *Environ. Sci. Technol.* 2024, 58, 12051−12061

Read Online

ACCESS | Metrics & More | Article Recommendations | Supporting Information

ABSTRACT: Germicidal ultraviolet light (GUV) systems are designed to control airborne pathogen transmission in buildings. However, it is important to acknowledge that certain conditions and system configurations may lead GUV systems to produce air contaminants including oxidants and secondary organic aerosols (SOA). In this study, we modeled the formation and dispersion of oxidants and secondary contaminants generated by the operation of GUV systems employing ultraviolet C 254 and 222 nm. Using a three-dimensional computational fluid dynamics model, we examined the breathing zone concentrations of chemical species in an occupied classroom. Our findings indicate that operating GUV 222 leads to an approximate increase of 10 ppb in O_3 concentration and 5.2 $\mu g \cdot m^{-3}$ in SOA concentration compared to a condition without GUV operation, while GUV 254 increases the SOA concentration by about 1.2 $\mu g \cdot m^{-3}$, with a minimal impact on the O_3 concentration. Furthermore, increasing the UV fluence rate of GUV 222 from 1 to 5 $\mu W \cdot cm^{-2}$ results in up to 80% increase in the oxidants and SOA concentrations. For GUV 254, elevating the UV fluence rate from 30 to 50 $\mu W \cdot cm^{-2}$ or doubling the radiating volume results in up to 50% increase in the SOA concentration. Note that indoor airflow patterns, particularly buoyancy-driven airflow (or displacement ventilation), lead to 15−45% lower SOA concentrations in the breathing zone compared to well-mixed airflow. The results also reveal that when the ventilation rate is below 2 h^{-1}, operating GUV 254 has a smaller impact on human exposure to secondary contaminants than GUV 222. However, GUV 254 may generate more contaminants than GUV 222 when operating at high indoor O_3 levels (>15 ppb). These results suggest that the design of GUV systems should consider indoor O_3 levels and room ventilation conditions.

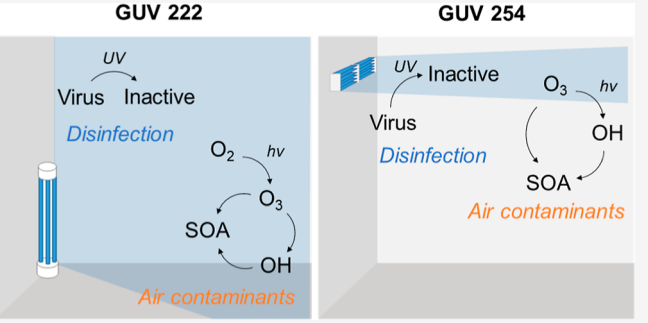

KEYWORDS: *indoor air quality, secondary organic aerosol (SOA), secondary chemistry, ventilation, ozone*

1. INTRODUCTION

In the 1800s, it was discovered that sunlight prevents the growth of microorganisms. Later, Wells and Fair demonstrated that ultraviolet C (UVC) inactivates airborne microorganisms.[1] UVC light functions by damaging the genetic materials (DNA or RNA) of infectious agents such as bacteria, viruses, and fungi, thus impeding their ability to replicate.[2,3] With the development of low-pressure mercury vapor lamps emitting UVC light in the mid-20th century, germicidal ultraviolet light (GUV) systems were utilized to prevent the spread of measles.[1] In the aftermath of the emergence of the novel Coronavirus (SARS-CoV-2), there has been a heightened interest in the effectiveness of GUV systems in killing airborne pathogens, positioning them as a cost-effective technology for airborne infection control.[4−7] Traditionally, UVC devices emitting light at a wavelength of 254 nm are employed as upper-room systems, targeting the upper part of a room due to their potential to cause harm to human skin cells and eyes.[3,8] In this setup, disinfection primarily occurs in the room's upper zone, with the airflow transporting airborne pathogens from the occupied zone to the upper zone, which plays a vital role in the disinfection performance.[9,10] More recently, UVC devices emitting light at a lower wavelength, specifically 222 nm, have emerged. Unlike UVC at 254 nm, UVC at 222 nm has the capability to irradiate the entire occupied zone, as it is known that UVC light ranging from 207 to 222 nm is relatively safe for human skin and eyes, while still possessing germicidal properties.[11]

GUV systems are commonly employed to control airborne pathogen transmission. However, it is imperative to recognize that they may inadvertently introduce air contaminants. For example, UVC at 254 nm generates gas-phase hydroxyl (OH) radicals through ozone photolysis, while UVC at 222 nm produces O_3 through oxygen photolysis.[12−21] These potent oxidants are inherently harmful to humans and initiate indoor

Received: January 16, 2024
Revised: May 9, 2024
Accepted: June 13, 2024
Published: June 26, 2024

gas phase chemistry with volatile organic compounds (VOCs) in occupied spaces.[22,23] Subsequent chemical reactions can give rise to the formation of oxygenated volatile organic compounds (OVOC) and secondary organic aerosols (SOA), both of which can detrimentally impact human health.[17,24−26] Furthermore, the heightened usage of chlorine-based disinfection products due to COVID-19 can introduce additional VOCs indoors that readily react with oxidants produced by UVC devices.[21,27,28]

GUV systems and air cleaning devices utilizing UVC lights can produce gas-phase oxidation products and increase particle concentrations indoors.[20,21,29] Both modeling study[21] and laboratory measurements[30−32] have shown that the operation of UVC 222 nm devices is associated with increasing indoor O_3 and particle concentrations. Moreover, in a laboratory setting, the deployment of one hospital-grade 254 nm was observed to increase particle number concentrations from 10^3 to 10^5 particles·cm^{-3}, representing a 2 orders of magnitude increase compared to the background.[20] However, despite these findings, there is limited information available about how GUV systems and various ventilation conditions, such as ventilation strategies and supply flow rates, influence the distribution of secondary contaminants generated by GUV systems, particularly within the human breathing zone. To fill these knowledge gaps, the objective of this study is to model and examine the formation and transport of oxidants and secondary contaminants in a ventilated occupied classroom, considering GUV system operating conditions and ventilation scenarios. Moreover, a three-dimensional computational fluid dynamics (CFD) simulation is utilized to investigate the intricate effects of indoor airflow on the spatial distribution of contaminants, which cannot be explored using a well-mixed box model. The findings elucidate how chemical processes linked to the GUV system are influenced by factors such as UV intensity (UV fluence rate), the radiating volume of UVC at 254 nm, ventilation conditions, and outdoor O_3 concentration.

2. METHODS

2.1. CFD Model. Figure 1 illustrates the study domain, representing the classroom geometry with dimensions of 7.7 × 7.7 × 3.0 m (length × width × height). The classroom was simulated with one speaker and 20 students, based on the occupant density for the classroom recommended by ASHRAE standard 62.1.[33] Two representative ventilation conditions were considered: (1) mixing ventilation and (2) displacement ventilation. For mixing ventilation, air jets were supplied through four-way ceiling diffusers angled at 30° toward the ceiling. In the case of displacement ventilation, low-momentum air was supplied through a diffuser located at the bottom of the wall. The total areas of supply air for mixing and displacement ventilations were 0.3 and 0.8 m^2, respectively, with an exhaust outlet area of 0.4 m^2. In the baseline scenario, the ventilation rate was set at 2 h^{-1}, equivalent to 360 m^3·h^{-1} with 100% outdoor air, in accordance with the minimum required ventilation rate by ASHRAE standard 62.1.[33] The supply air temperature was configured at 14 °C for mixing ventilation and 18 °C for displacement ventilation, considering occupant thermal comfort.[34] Each occupant's metabolic heat of 99 W was apportioned into 40% for the convective load and 60% for the radiative load.[35] The convective load was applied to the human surface as a convective heat flux, while the radiative load was distributed to surrounding surfaces (wall, floor, and ceiling).[36] To simulate a talking mode, the air jet

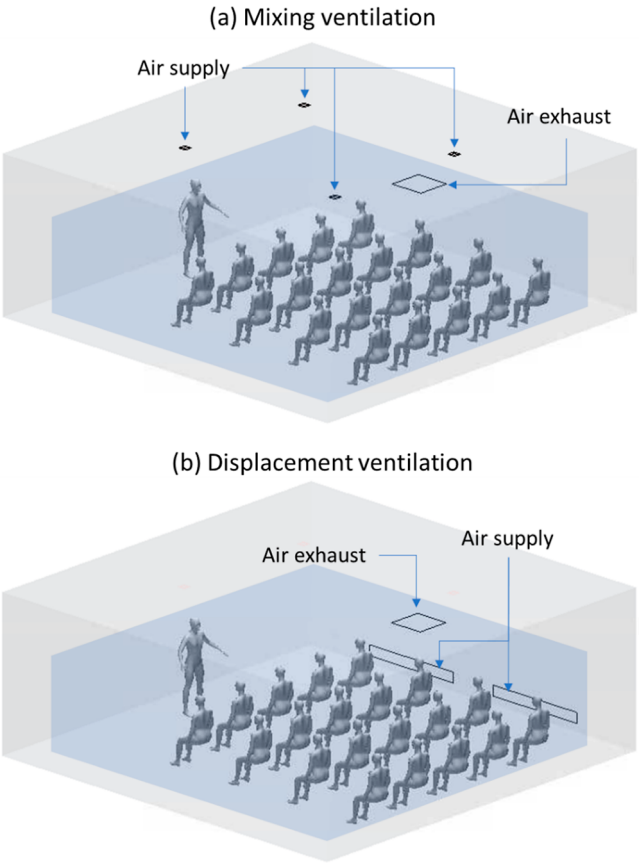

Figure 1. Classroom geometry for the CFD simulation: (a) mixing ventilation and (b) displacement ventilation. Note that the blue box represents the ASHRAE breathing zone defined as the air volume ranging from 7.6 to 180 cm above the floor and 60 cm away from the walls.

speed from the speaker's 2 cm^2 mouth opening was set at 2 m·s^{-1}, with an air temperature of 34 °C.[37,38]

The indoor airflow fields were calculated using a commercial CFD solver, STAR-CCM+ version 2021.03. A steady-state gas transport model was employed to simulate the indoor chemical reactions associated with photochemistry. Note that in this study, SOA was modeled based on chemical reactions 1, 2, and 4 (see Table 1), as a continuous gas-phase. Since the buoyancy-driven convective thermal plume near heat sources plays an important role in the turbulent airflow near a human body, the Reynolds averaged Navier−Stokes model with the shear stress transport k−ω model was used.[39,40] The details of the mesh generation and convergence check are described in the Supporting Information (see the Supporting Information CFD model setup).

The simulation involved solving a three-dimensional convection-diffusion equation to examine the transport of gas-phase compounds, while accounting for chemical reactions, as shown below

$$\frac{\partial}{\partial t}(\rho C_i) + \frac{\partial}{\partial x}(\rho u C_i) = \frac{\partial}{\partial x}\left(\rho D \frac{\partial C_i}{\partial x}\right) + S_i + R_i \quad (1)$$

where ρ is the density of air, C_i is the mole fraction of chemical species, u is the velocity of air, D is the molecular diffusion coefficient; S_i is the source term or sink term (i.e., emission of chemical species or ozone deposition), and R_i is the chemical reaction term. In the simulation, R_i is defined as follows[25]

https://doi.org/10.1021/acs.est.4c00575
Environ. Sci. Technol. 2024, 58, 12051−12061

Table 1. Chemical Reactions Applied in the CFD Model

no	reactants		products		rate constant ($cm^3 \cdot mol^{-1} \cdot s^{-1}$)	references
R1	limonene	O_3	0.86 OH	SOA	2.1×10^{-16}	21,30
R2	limonene	OH	SOA		1.6×10^{-10}	41
R3	VOCs	OH	OVOC		8.1×10^{-12}	30
R4	OVOC	OH	SOA		8.1×10^{-12}	30
R5	O_3	OH	HO_2	O_2	7.3×10^{-14}	30,44
R6	HO_2	OH	H_2O	O_2	1.1×10^{-10}	30,44
R7	NO_2	OH	HNO_3		2.5×10^{-11}	45
R8	CO	OH	CO_2	HO_2	2.4×10^{-13}	46
R9	HO_2	O_3	OH	$2O_2$	2.0×10^{-15}	30,44
R10	NO	HO_2	OH	NO_2	8.1×10^{-12}	46
R11	$2HO_2$		H_2O_2	O_2	1.7×10^{-12}	44,47
R12	O_3	NO	O_2	NO_2	1.8×10^{-14}	44

Table 2. Photochemistry by UVC 222 and 254 nm

	reactants		products		room-averaged UV fluence rate ($\mu W \cdot cm^{-2}$)	UV flux (photons $cm^{-2} \cdot s^{-1}$)
UVC 222 nm	O_2		O_3		1	1.1×10^{12}
					3	3.4×10^{12}
					5	5.6×10^{12}
UVC 254 nm	O_3	H_2O	OH	O_2	30	3.8×10^{13}
					40	5.1×10^{13}
					50	6.4×10^{13}

$$R_i = M_i \sum_{r=1}^{N} R_{i,r} \quad (2)$$

where M_i is the molecular weight of ith species, N_r is the number of chemical reactions, and $R_{i,r}$ is the molar rate of generation or loss of ith species in the reaction r. The reaction term is the net production and consumption rate due to chemical reactions for each chemical component in the air.

2.2. Indoor Chemistry Modeling. In this study, a total of 12 chemical reactions were modeled to describe the generation of oxidants and SOA (see Table 1). It is noteworthy that limonene ozonolysis (R1) is a primary reaction producing OH,[21,30] and R2 is the limonene reaction with OH that produces SOA.[41] The rate constants for R1 and R2 were calculated assuming an indoor temperature of 295 K.[41,42] R3 is the reaction generating OVOC and OH, while the reaction between OVOC and OH leads to the production of SOA (R4).[30,43] To calculate the rate constants of the VOCs and OH reaction, the rate constants are multiplied by the mole fraction to establish a weighted average OH rate constant for the VOC mixture (R3). It is assumed that the reactivity of the OH reaction with OVOC is the same as that of the OH reaction with VOCs.[30] R5−R12 describe the reactions involving O_3, OH, HO_2, and major combustion products from outdoors, such as NO, NO_2, and CO.[30,44−47]

Given that the primary source of O_3 is outdoors,[48] we assume that indoor background O_3 was solely introduced from outdoor sources, with a concentration of 40 ppb based on typical ambient O_3 concentrations in urban areas.[49,50] Indoor O_3 removal occurred through deposition on the room surfaces (surrounding walls, floor, and ceiling) at a total loss rate of 2.8 h^{-1},[51] as well as onto the human surfaces with a deposition velocity of 6.8 $m \cdot h^{-1}$ for laundered clothing.[25] Similarly, no indoor source of combustion products was considered, while the outdoor concentrations of NO, NO_2, and CO were set to 1, 10, and 1000 ppb, respectively, based on previous studies.[21,51] Taking into account furniture (such as desks and chairs) and the frequency of cleaning products usage in the classroom, a relatively high emission rate of VOCs from indoor surfaces was set at 150 $\mu g \cdot m^{-2}\ h^{-1}$.[52] The occupants served as strong sources of VOCs and limonene, with emission rates set at 1 $\mu g \cdot s^{-1}$ $person^{-1}$.[53,54] We also assumed that all chemical reactions occur at an atmospheric pressure of 1 atm and a relative humidity of 35−40%, which is typical of indoor environments at sea level.

UVC radiation with wavelengths shorter than 242 nm dissociates O_2 into two oxygen atoms. These highly reactive oxygen atoms can subsequently combine with other O_2 molecules to produce O_3.[31] In the case of UVC 254 nm, the UVC light photolyzes O_3 into O (^1D) and O_2 with the subsequent reaction between singlet oxygen (O(^1D)) and H_2O, producing two OH radicals.[55] Note that the OH yield from the O_3 photolysis and O (^1D) and H_2O reaction is about 0.2 due to quenching of O (^1D) to O (^3P).[56] Table 2 outlines the detailed photochemistry associated with UVC 222 and 254 nm.

UV fluence rates were selected based on recommendations from the U.S. Center for Disease Control (CDC) for GUV 254 and previous studies examining GUV 222.[30−32,57,58] Note that we assumed that there is no O_3 generation by UVC at 254 nm, nor did we consider the effect of UV light through windows. GUV 254 and GUV 222 have four wall-mounted and ceiling-mounted UV fixtures, respectively (see Table S2). The spatial distributions of the fluence rate created by GUV 254 and 222 were calculated using the Visual Software available at https://www.acuitybrands.com/resources/technical-resources/visual-lighting-software.[10] Wall-mounted fixtures (GUV 254) generate broad, flat beams directed horizontally and above the horizontal plane, while ceiling-mounted fixtures (GUV 222) produce 120° beams irradiating the entire room. The power of each UV fixture was set to achieve the desired room-average UV fluence rate, as detailed in Table 2.

2.3. CFD Model Validation. To ensure the reliability of our CFD model, we conducted the model validation to assess

https://doi.org/10.1021/acs.est.4c00575
Environ. Sci. Technol. 2024, 58, 12051−12061

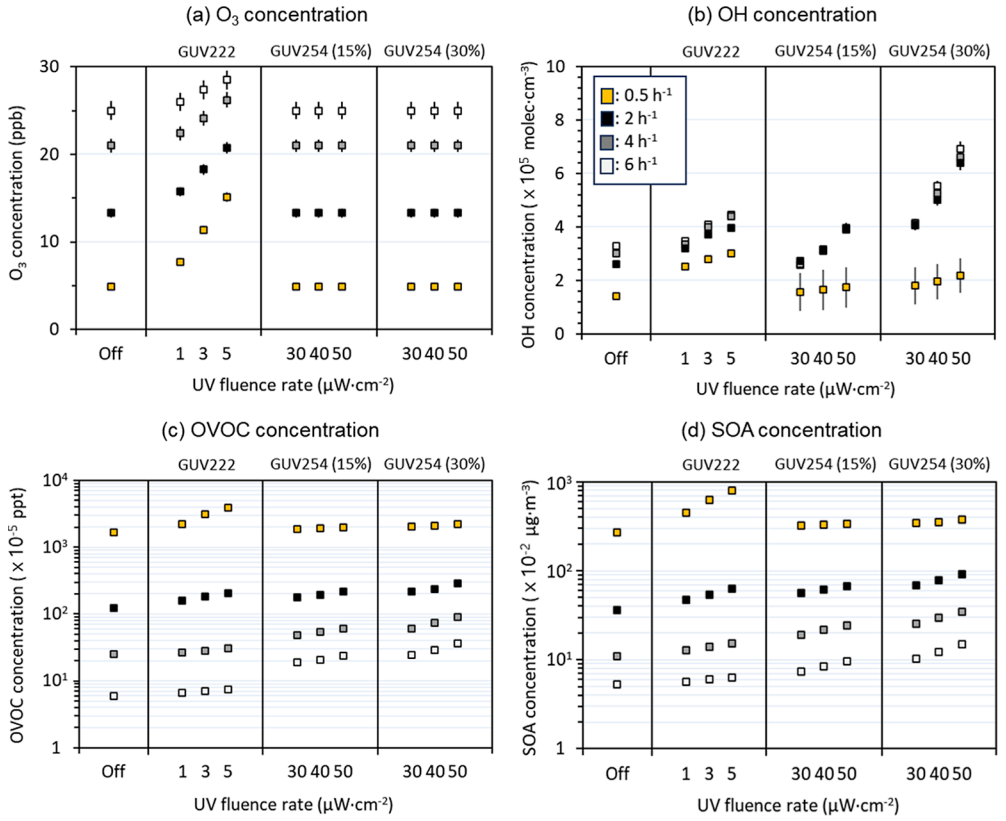

Figure 2. Breathing zone (a) O_3, (b) OH, (c) OVOC, and (d) SOA concentrations under mixing ventilation. Note that the outdoor O_3 concentration is 40 ppb, and the error bars represent the standard deviation. (c) OVOC and (d) SOA concentrations have a logarithmic scale on a *y*-axis.

its capability in predicting (1) the nonuniform airflow field and particle transport, (2) O_3 generation by the GUV system, and (3) O_3 deposition on the indoor surfaces. Moreover, sensitivity analyses were performed, considering both low- and high emission scenarios for VOCs and limonene.

In the first step, we validated the airflow field by comparing the velocity profiles within a simulated room with CFD simulations and experimental results. The CFD model and boundary conditions were aligned with the experimental setup by Liu et al. (2022).[59] Figures S2 and S3 illustrate the vertical air velocity and particle concentration profiles considering mixing and displacement ventilation conditions. For mixing ventilation, the difference between the CFD simulation and experiment was observed to be less than 0.03 $m{\cdot}s^{-1}$ (mean difference of 15%). This relatively minor difference can be attributed to the enhanced mixing effect associated with mixing ventilation, resulting in a relatively uniform airflow velocity throughout the room. In contrast, under displacement ventilation, where low momentum air is supplied at floor height, the difference between the CFD simulation and experiment can reach 0.02 $m{\cdot}s^{-1}$ (mean difference of 39%). While the simulated results did not perfectly match the experimental data, the simulation effectively captures the general pattern of vertical air velocity profiles observed in experimental data. Moreover, Figures S4 and S5 show that the CFD simulation produces results with mean particle concentration differences of less than 15% under mixing ventilation and 33% under displacement ventilation compared to the experiment.[10] Note that particles were modeled by using the Eulerian approach with a size of 0.4 μm. While the simulation may not precisely align with the experiment, these results suggest that the CFD modeling approach employed in our study can be capable of predicting the airflow field and mass transport within the ventilated room.

Second, to validate the CFD simulation's capacity in modeling chemical reactions, we compared the O_3 concentrations computed by the CFD model (under mixing ventilation) during the operation of GUV 222 with experimental data from Barber et al. (2023).[20] Figure S6 illustrates good agreement between the concentration of O_3 calculated by the CFD model and the experimental results, confirming that the CFD model can provide meaningful insights into indoor chemical reactions and photochemistry.

Third, we compared the O_3 concentrations calculated by the CFD model (mixing ventilation) with those derived from the mass balance model (eq 3).[60] This assessment aimed to evaluate the CFD model's capability to predict the O_3 deposition in indoor surfaces and the generation of O_3 by GUV 222. For this purpose, we examined two representative scenarios: (1) GUV off and (2) GUV 222 on.

$$\frac{dC_{in}(t)}{dt} = aC_{out}(t) - (a + k)C_{in}(t) + \frac{E(t)}{V} \quad (3)$$

where $C_{in}(t)$ is the indoor O_3 concentration at time, t (ppb), $C_{out}(t)$ is the outdoor O_3 concentration at time, t (ppb), a is the air change rate (h^{-1}), k is the O_3 deposition rate (h^{-1}), $E(t)$ is the emission rate at time t ($\mu g{\cdot}h^{-1}$), and V is the total room volume (m^3). Note that for the mass balance model, the O_3 generation by GUV 222 was calculated based on the photolysis of the O_2 photolysis. The photolysis rate of UVC 222 nm was estimated as 1.4×10^{-11} s^{-1} using a UV flux of 3.4

https://doi.org/10.1021/acs.est.4c00575
Environ. Sci. Technol. 2024, 58, 12051−12061

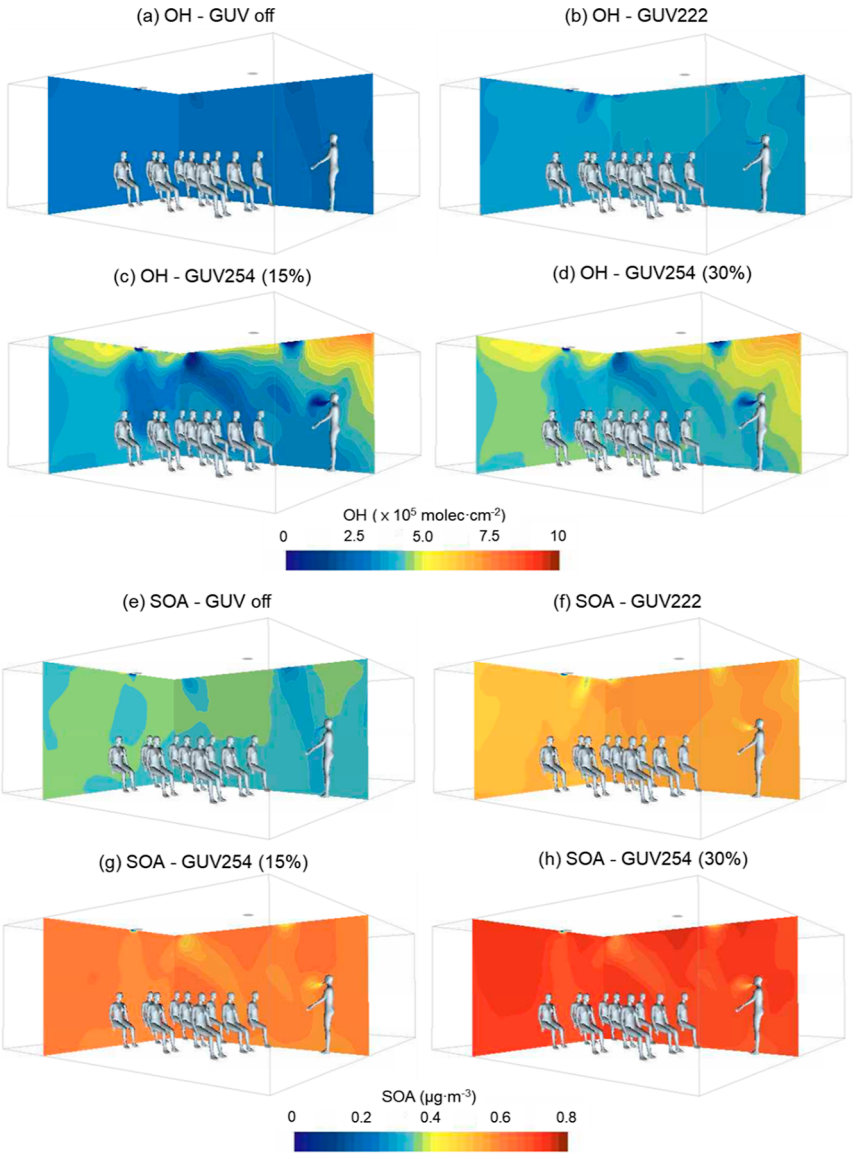

Figure 3. Spatial distribution of OH (a–d) and SOA (e–h) concentrations under mixing ventilation. Note that the outdoor O_3 concentration is 40 ppb, and the ventilation rate is 2 h^{-1}.

$\times 10^{12}$ $cm^{-2}\cdot s^{-1}$ (see Table 2), an absorption cross section of 4.1×10^{-24} cm^2, and a quantum yield of 1.[31]

Figure S7 illustrates the room average O_3 concentrations obtained from both the CFD model and the mass balance model for mixing ventilation at a ventilation rate of 2 h^{-1}. The CFD model results demonstrate a good agreement with the mass balance model results across test cases. Furthermore, the CFD model yields a consistent trend in indoor O_3 concentrations, indicating that the indoor concentration is 60 to 70% lower than the outdoor concentration.[61]

Lastly, a sensitivity analysis was conducted for SOA formation considering both low and high levels of VOCs and limonene emissions. According to Table S3, when occupants emit different levels of limonene and VOCs (×0.1, ×2 and ×10), the SOA concentration increases proportionally to the elevated emissions, reaching up to 6.1 $\mu g\cdot m^{-3}$, while maintaining similar fractions of SOA components.

2.4. Parametric Analysis. We conducted a parametric analysis to investigate the effects of GUV system operating conditions (UV fluence rate and radiating volume), ventilation conditions (ventilation rate and strategy), and outdoor O_3 concentrations on the formation of oxidants and secondary contaminants by GUV systems. For UVC 222 nm, three different UV fluence rates (1, 3, and 5 $\mu W\cdot cm^{-2}$) were examined, while for UVC 254 nm, three different UV fluence rates (30, 40, and 50 $\mu W\cdot cm^{-2}$) and two radiating volumes (15 and 30% of the total room volume) were tested.[30−32,57,58]

Regarding ventilation conditions, we explored mixing ventilation and displacement ventilation. These two ventilation strategies create distinct room airflow patterns, influencing the transport of indoor contaminants near occupants.[10,34,59,62] Mixing ventilation is commonly employed in mechanically ventilated buildings with ceiling diffusers, while displacement ventilation is common in residential or naturally ventilated spaces, where low-momentum air is supplied at the room floor level, generating an upward airflow pattern with minimal mixing effects. Moreover, as ventilation rate affects the removal effect of indoor air contaminants, we considered four ventilation rates: 0.5 h^{-1} (insufficient ventilation), 2 h^{-1} (the baseline, the minimum requirement by ASHRAE standard

https://doi.org/10.1021/acs.est.4c00575
Environ. Sci. Technol. 2024, 58, 12051−12061

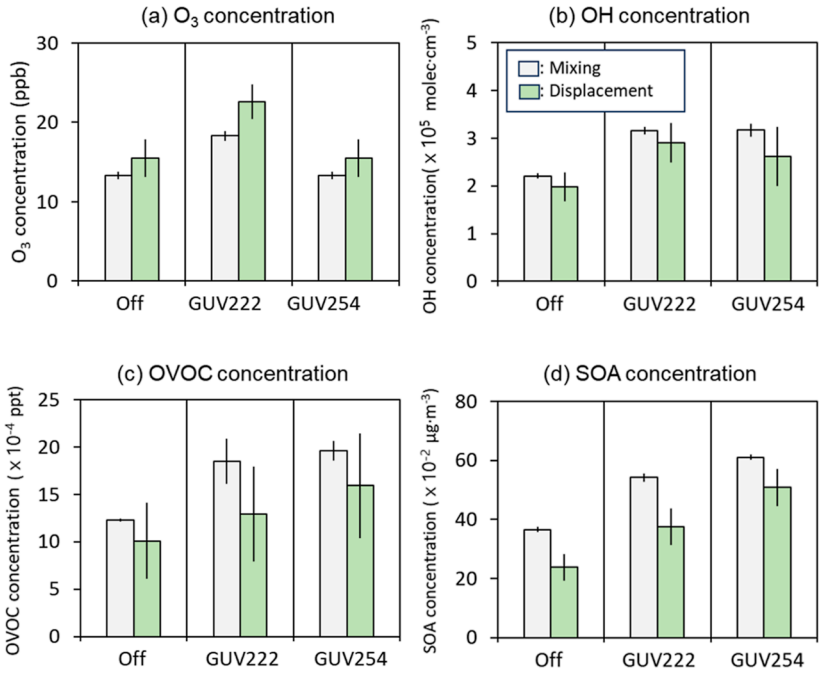

Figure 4. Breathing zone (a) O_3, (b) OH, (c) OVOC, and (d) SOA concentrations under mixing and displacement ventilations at a ventilation rate of 2 h^{-1}. The outdoor O_3 concentration is 40 ppb, and the UV fluence rate is 3 $\mu W \cdot cm^{-2}$ for GUV 222 and 40 $\mu W \cdot cm^{-2}$ for GUV 254 with a radiating volume of 15%. Note that the error bars represent the standard deviation.

62.1), 4 h^{-1} (good level by Lancet) and 6 h^{-1} (better level by Lancet).[33,63]

Since the O_3 concentration can play a crucial role in forming SOA, we considered three outdoor O_3 concentrations (10, 40, and 80 ppb) to assess the effect of the outdoor O_3 levels. These values were chosen to represent the minimum, average, and maximum ambient O_3 concentrations typically found in large cities.[49,50] Using these concentrations, the average concentrations were calculated for the ASHRAE breathing zone, defined as the air volume ranging from 7.6 to 180 cm above the floor and 60 cm away from the walls[33] (see Figure 1).

3. RESULTS

3.1. Effects of GUV Operating Conditions. Figure 2 illustrates the mean ASHRAE breathing zone concentrations of O_3, OH, OVOC, and SOA under representative GUV system operating conditions and ventilation rates for mixing ventilation. Note that the outdoor concentration of O_3 is 40 ppb. Figure 2c,d utilizes a logarithmic scale on the *y*-axis. The molar mass of SOA is assumed to be 200 g·mol^{-1}.[21] Table S4 provides a comprehensive summary of all the results presented in Figure 2.

According to the figure, in the absence of GUV operation, indoor O_3 concentration remains 40−90% lower than outdoor levels, primarily due to the indoor O_3 deposition onto indoor surfaces, with an approximate total first-order decay rate of 4 h^{-1} (2.8 h^{-1} for wall surfaces and 1.2 h^{-1} for human surfaces).[25,51] With an increased ventilation rate, more O_3 infiltrates indoors, resulting in a rise in O_3 concentration (see Figure 2a). The higher ventilation rate also leads to an elevated OH concentration, attributed to the predominant impact of limonene and VOCs ozonolysis on OH generation (Figure 2b). In contrast, OVOC and SOA concentrations have a negative correlation with the ventilation rate (Figure 2c,d). For instance, the SOA concentration is reduced by about 98% as the ventilation rate increases from 0.5 to 6 h^{-1}. This decline is ascribed to the more potent removal effect of ventilation, which outweighs the generation of these compounds through chemical reactions. However, under low ventilation rates, where more VOCs and limonene are present indoors (Figure S8), there is an increased likelihood for O_3 and OH radicals to undergo chemical reactions with VOCs and limonene.

Figure 2a shows that the operation of GUV 222 elevates the concentration of the O_3 by up to 10 ppb. The calculated O_3 generation rate for GUV 222 at a UV fluence rate of 3 $\mu W \cdot cm^{-2}$ is 30 ppb·h^{-1}, consistent with previous studies.[31,32] The amount of O_3 produced by GUV 222 is proportional to the UV fluence rate as a higher UV flux amplifies the photochemical reaction. Accordingly, concentrations of OH, OVOC, and SOA increase when GUV operates with a higher UV fluence rate (Figure 2b−d). It is noteworthy that at a ventilation rate of 0.5 h^{-1}, operating GUV 222 with a UV fluence rate of 5 $\mu W \cdot cm^{-2}$ results in a notable increase in the SOA concentration, reaching 7.9 $\mu g \cdot m^{-3}$. This is three times higher than the concentration observed when GUV is inactive. Even at the minimum ventilation rate by ASHRAE standard 62.1 (2 h^{-1}),[33] GUV 222 operation still significantly impacts, resulting in a significant increase of up to 70% in SOA concentration (from 0.37 to 0.62 $\mu g \cdot m^{-3}$). However, as the ventilation rate exceeds 4 h^{-1}, this impact diminishes to 10−30%.

GUV 254 operation has a negligible effect on indoor O_3 concentration, as the O_3 generation is modeled solely through the photolysis of UVC 222 nm (see Figure 2a and Tables 1 and 2). Previous studies also showed that UVC 254 nm marginally increases indoor O_3 concentration.[20,21] On the other hand, the operation of GUV 254 significantly affects the OH concentration in the breathing zone (see Figures 2b and 3c,d). When GUV 254 irradiates 15% of the total room volume, the OH concentration in the breathing zone increases to 3.94 × 10^5 molec·cm^{-3}. Doubling the radiated volume to 30% results in a concentration surge of up to 6.93 × 10^5 molec·

https://doi.org/10.1021/acs.est.4c00575
Environ. Sci. Technol. 2024, 58, 12051−12061

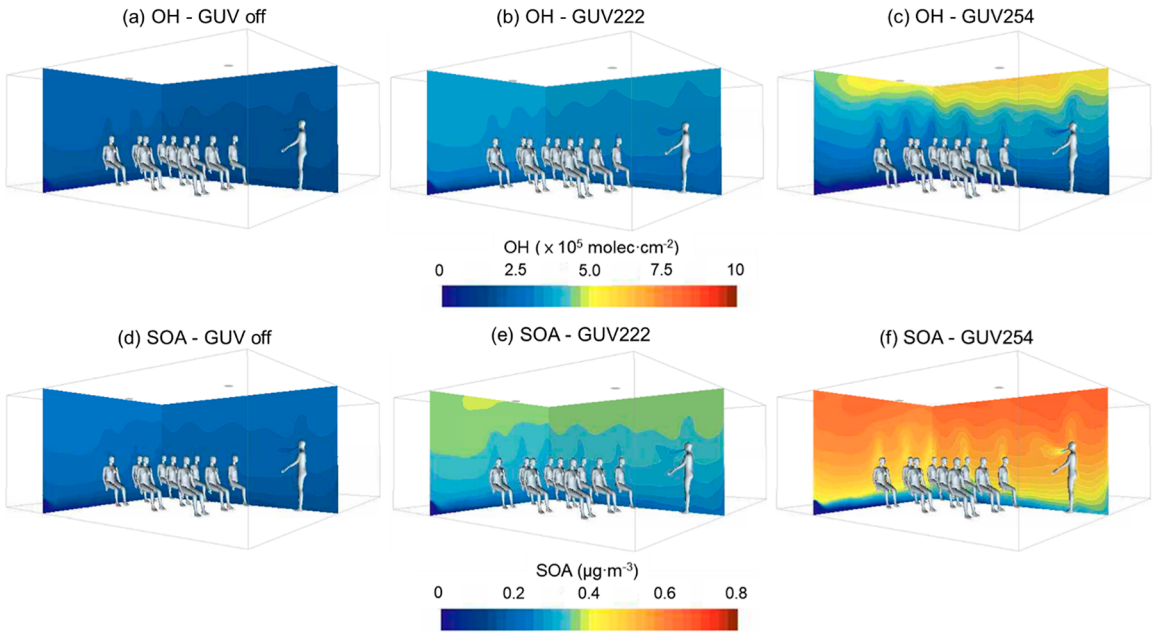

Figure 5. Spatial distribution of OH (a–c) and SOA (d–f) concentrations under displacement ventilation at a ventilation rate of 2 h^{-1}. Note that the outdoor O_3 concentration is 40 ppb, and the UV fluence rate is 3 $\mu W \cdot cm^{-2}$ for GUV 222 and 40 $\mu W \cdot cm^{-2}$ for GUV 254 with a radiating volume of 15%.

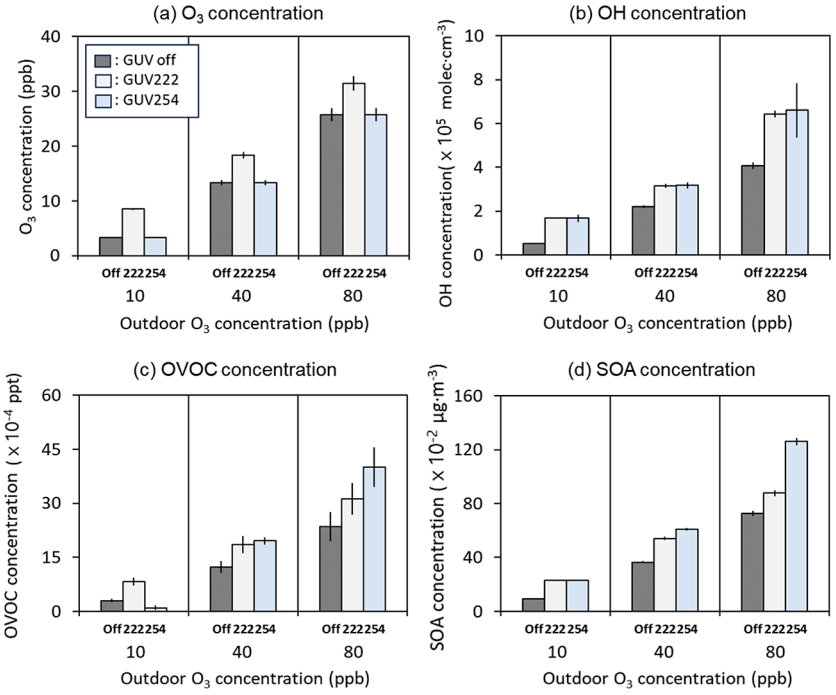

Figure 6. Breathing zone (a) O_3, (b) OH, (c) OVOC, and (d) SOA concentrations under mixing at a ventilation rate of 2 h^{-1}. UV fluence rate is 3 $\mu W \cdot cm^{-2}$ for GUV 222 and 40 $\mu W \cdot cm^{-2}$ for GUV 254 with a radiating volume of 15%. Note that the error bars represent the standard deviation.

cm^{-3}. In a poorly ventilated condition (at 0.5 h^{-1}), GUV 254 increases SOA concentration by about 1.2 $\mu g \cdot m^{-3}$ from the background (see Figure 2d). However, compared to GUV 222, the influence of GUV 254 on SOA formation becomes more pronounced as the ventilation rate increases. This is primarily due to UVC at 254 nm producing more OH radicals as additional outdoor O_3 is introduced indoors.

Figure 3c,d indicates that a high OH concentration is formed on the upper part of the room where UVC at 254 nm irradiates. However, SOA formed by UVC 254 nm is distributed relatively evenly within a room, primarily due to the longer residence time of SOA and the air mixing facilitated by mixing ventilation (see Figure 3g,h).[10,34,47] This trend arises from the reactivity of OH radicals, which undergo rapid reactions with indoor limonene or VOCs, occurring on a much faster time scale than the transport time scale (7–15 $cm \cdot s^{-1}$ based on the room average airspeed).[46,47,64]

3.2. Effects of Ventilation Strategy. Figure 4 depicts the breathing zone concentrations of the ligands of the O_3, OH, OVOC, and SOA under mixing and displacement ventilations

https://doi.org/10.1021/acs.est.4c00575
Environ. Sci. Technol. 2024, 58, 12051–12061

at a ventilation rate of 2 h^{-1}. Note that the outdoor O_3 concentration is 40 ppb, and the UV fluence rate is 3 $\mu W \cdot cm^{-2}$ for GUV 222 and 40 $\mu W \cdot cm^{-2}$ for GUV 254 with a radiating volume of 15%. The figure reveals that the breathing zone O_3 concentration under displacement ventilation is 15.5 ppb, which is 20% higher than that under mixing ventilation. In displacement ventilation, outdoor air is introduced through the inlet near the floor, leading to a higher O_3 concentration observed in the lower part of the room (i.e., the breathing zone). In contrast, mixing ventilation exhibits a relatively uniform O_3 distribution due to its mixing effect (see Figure S9).

The enhanced air mixing effect also contributes to a relatively uniform OVOC and SOA distribution throughout the room (see Figures 3 and S10), while under displacement ventilation, the thermally stratified airflow transports air contaminants to the upper part of the room[34,62,65,66] (see Figures 5, S10, and S11). Such airflow pattern results in 15−30% lower OVOC and SOA concentrations within the breathing zone than mixing ventilation, while concentrations are relatively high above the breathing zone. This concentration difference between mixing and displacement ventilation grows to 45% as the ventilation rate increases from 2 to 6 h^{-1} (see Figures S12 and S13). Under displacement ventilation, supply air is displaced upward more effectively without air mixing, especially with increased air supply.[10,66] Consequently, the concentration difference between the breathing zone and the upper part of the room is amplified by higher ventilation rates.

3.3. Effects of Outdoor O_3 Concentration. Figure 6 presents the breathing zone concentrations of O_3, OH, OVOC, and SOA as a function of the outdoor O_3 concentration. Mixing ventilation is employed with a ventilation rate of 2 h^{-1}, and the UV fluence rate is 3 $\mu W \cdot cm^{-2}$ for GUV 222 and 40 $\mu W \cdot cm^{-2}$ for GUV 254 with a radiating volume of 15%.

In Figure 6a, GUV 222 induces an increase in the O_3 concentration of approximately 5−6 ppb because of the formation of O_3 from the oxygen photolysis. Notably, the impact of O_3 generation by GUV 222 becomes relatively pronounced when the outdoor O_3 concentration is lower (at 10 ppb). However, the impact of O_3 generated by GUV 222 on indoor air contaminants concentration diminishes as the outdoor O_3 concentration rises from 10 to 80 ppb.

UVC at 254 nm directly decomposes O_3 into OH, resulting in more generations of OH, OVOC, and SOA, particularly at higher outdoor O_3 concentrations (see Figure 6b−d). As the outdoor O_3 concentration escalates from 10 to 40 ppb, GUV 254 results in an approximately 370% increase in SOA concentration at a ventilation rate of 2 h^{-1}. Note that the impact of GUV 254 on SOA formation outweighs that of GUV 222 at an outdoor O_3 concentration of 80 ppb and higher ventilation rates (4 and 6 h^{-1}), as more O_3 is introduced indoors (see Figures S14 and S15).

4. DISCUSSION

We investigated the generation of undesired air contaminants by GUV systems (GUV 222 and 254) in a populated classroom. Our results, derived from simulated environmental conditions, highlight the important role of UVC intensity and its radiating volume in secondary contaminant formation by GUV systems. For example, elevating the UV fluence rate from 1 to 5 $\mu W \cdot cm^{-2}$ for GUV 222 can result in a 100% increase in oxidants (e.g., from 7.7 to 15.1 ppb) and SOA concentration (from 4.5 to 7.9 $\mu g \cdot m^{-3}$) when ventilation is insufficient (0.5 h^{-1}). This finding suggests that while increasing the UV fluence rate may be beneficial for controlling airborne pathogens,[3,57] particularly in poorly ventilated settings, it may potentially result in higher human exposure to air contaminants produced by GUV 222.[30,32] With regard to GUV 254, increasing the UV fluence rate from 30 to 50 $\mu W \cdot cm^{-2}$ or doubling the radiating volume results in up to about 50% increase in SOA concentration. This is because augmenting the UV fluence rate and radiating volume of GUV 254 increases the generation of OH radicals, thereby promoting the formation of secondary contaminants, especially in environments with elevated indoor O_3 levels.

Previous studies reported that in typical indoor settings, the impact of GUV 254 on the formation of secondary contaminants is not substantial, whereas GUV 222 demonstrates more notable effects, especially under inadequately ventilated conditions.[21,67] This study further reveals that it also depends on indoor O_3 levels, mainly determined by the outdoor O_3 concentration and ventilation rate. For example, when the indoor O_3 concentration is higher than 15 ppb, the operating GUV 254 can generate more SOA than GUV 222.

In addition to the GUV operating condition, the indoor airflow pattern also has a notable effect on the breathing zone SOA concentration. The presence of thermally stratified airflow brings distinct advantages in lowering OVOC and SOA concentrations within the human breathing zone. This is mainly because stratified airflow directs air contaminants above the breathing zone without air mixing, whereas mixing ventilation uniformly distributes air contaminants throughout the space.[65,66] Furthermore, the well-mixed distribution of reactants is likely to increase collision frequency between molecules and facilitate chemical reactions.[68,69] However, it is worth noting that air mixing is crucial for GUV 254 systems to disinfect airborne pathogens;[10,57,70] previous studies show that mixing ventilation improves disinfection performance by approximately 20% compared to displacement ventilation. This is particularly important in environments characterized by random infection spread and high population density.

Taken together, our findings suggest that the UV intensity and radiating volume of GUV systems should be carefully designed considering indoor O_3 level and ventilation conditions, especially for poorly ventilated conditions (e.g., naturally ventilated classrooms). Operating GUV systems with minimal fluence rates and radiating volumes while ensuring effective disinfection tailored to the specific needs of a given space is highly advisible. Moreover, it is essential to acknowledge that occupied environments often experience heightened concentrations of particles and VOCs due to indoor activities.[71,72] In such scenarios, a layered approach, such as integrating O_3 scrubbers, can be contemplated to effectively remove pollutants that may contribute to SOA formation.[73] This multifaceted strategy not only enhances air quality but also promotes the overall efficacy of GUV systems in indoor disinfection.

While this study has established a CFD-modeling framework to study spatial distributions of chemical species associated with the GUV system, some limitations should be acknowledged. First, this study modeled chemical reactions mainly focusing on the transport and formation of secondary contaminants by GUV operating and ventilation conditions. The compositions of VOCs, radicals other than OH and HO_2, gas-surface partitioning of OVOC, and chemical reactions

https://doi.org/10.1021/acs.est.4c00575
Environ. Sci. Technol. 2024, 58, 12051−12061

related to human skin oils were not considered. Second, our investigation did not explore the variations in the relative humidity and temperature. They can impact the formation of O_3 and SOA as well as the volatility of VOCs indoors,[21,74,75] although indoor environmental conditions of mechanically ventilated rooms are relatively consistent compared to outdoors.[76] Third, this study is based on steady-state gas phase analysis with constant rate coefficients. Accordingly, particle coagulation, gas-particle partitioning, deposition, and vapor wall loss effects of SOA are not accounted for in this modeling study. Lastly, the SOA mass yield from the chemical reactions is simplified; for example, SOA mass yield from limonene oxidation varies up to 20% with indoor settings.[21] Future studies are warranted to investigate further the impacts of humans on OH radicals and SOA formation as well as more detailed aerosol and composition analyses.

■ ASSOCIATED CONTENT

Supporting Information

The Supporting Information is available free of charge at https://pubs.acs.org/doi/10.1021/acs.est.4c00575.

CFD model setup, details of three mesh resolution sets, details of UV fixtures, formation of SOA with the different VOCs and limonene emission conditions, summary of the breathing zone O_3, OH, OVOC, and SOA concentrations under mixing ventilation, mesh view of mesh 2, comparison of the measured and simulated air velocity profiles under mixing ventilation, comparison of the measured and simulated air velocity profiles under displacement ventilation, comparison of the measured and simulated particle concentration under mixing ventilation, comparison of the measured and simulated particle concentration under displacement ventilation, comparison of O_3 concentrations predicted by the CFD model and the experiment, the room average O_3 concentrations calculated by the CFD model and mass balance model, breathing zone VOCs and limonene concentrations under mixing ventilation, spatial distribution of O_3 concentrations under mixing ventilation and displacement ventilation, spatial distribution of OVOC concentrations under mixing ventilation and displacement ventilation, spatial distribution of limonene concentrations under (a) mixing ventilation and (b) displacement ventilation at a ventilation rate of 2 h^{-1}, breathing zone O_3, OH, OVOC, and SOA concentrations under mixing and displacement ventilations at a ventilation rate of 4 h^{-1}, breathing zone O_3, OH, OVOC, and SOA concentrations under mixing and displacement ventilations at a ventilation rate of 6 h^{-1}, breathing zone O_3, OH, OVOC, and SOA concentrations under mixing at a ventilation rate of 4 h^{-1}, and breathing zone O_3, OH, OVOC, and SOA concentrations under mixing at a ventilation rate of 6 h^{-1} (PDF)

■ AUTHOR INFORMATION

Corresponding Author

Donghyun Rim − *Department of Architectural Engineering, Pennsylvania State University, University Park, Pennsylvania 16802, United States;* orcid.org/0000-0002-0751-3605; Phone: 1-814-863-2041; Email: dxr51@psu.edu

Authors

Seongjun Park − *Department of Architectural Engineering, Pennsylvania State University, University Park, Pennsylvania 16802, United States*

Youngbo Won − *Department of Architectural Engineering, Pennsylvania State University, University Park, Pennsylvania 16802, United States*

Complete contact information is available at: https://pubs.acs.org/10.1021/acs.est.4c00575

Notes

The authors declare no competing financial interest.

■ ACKNOWLEDGMENTS

This research was supported by the Alfred P. Sloan Foundation MOCCIE3(G-2020-13912) and the U.S. National Science Foundation (NSF grant 1944325).

■ REFERENCES

(1) Reed, N. G. The history of ultraviolet germicidal irradiation for air disinfection. *Publ. Health Rep.* **2010**, *125* (1), 15−27.

(2) Walker, C. M.; Ko, G. Effect of ultraviolet germicidal irradiation on viral aerosols. *Environ. Sci. Technol.* **2007**, *41* (15), 5460−5465.

(3) Kowalski, W. *Ultraviolet Germicidal Irradiation Handbook: UVGI for Air and Surface Disinfection*; Springer Science & Business Media, 2010.

(4) Srivastava, S.; Zhao, X.; Manay, A.; Chen, Q. Effective ventilation and air disinfection system for reducing coronavirus disease 2019 (COVID-19) infection risk in office buildings. *Sustain. Cities Soc.* **2021**, *75*, 103408.

(5) US Centers for Disease Control and Prevention (CDC). *Cleaning, Disinfection, and Ventilation*, 2022. https://www.cdc.gov/coronavirus/2019-ncov/community/clean-disinfect/index.html.

(6) Zhu, S.; Lin, T.; Wang, L.; Nardell, E. A.; Vincent, R. L.; Srebric, J. Ceiling impact on air disinfection performance of upper-room germicidal ultraviolet (UR-GUV). *Build. Environ.* **2022**, *224*, 109530.

(7) Wang, M. H.; Zhang, H. H.; Chan, C. K.; Lee, P. K. H.; Lai, A. C. K. Experimental study of the disinfection performance of a 222-nm Far-UVC upper-room system on airborne microorganisms in a full-scale chamber. *Build. Environ.* **2023**, *236*, 110260.

(8) Hessling, M.; Haag, R.; Sieber, N.; Vatter, P. The impact of far-UVC radiation (200−230 nm) on pathogens, cells, skin, and eyes-a collection and analysis of a hundred years of data. *GMS Hyg. Infect. Control* **2021**, *16*, Doc07.

(9) Park, S.; Mistrick, R.; Rim, D. Performance of upper-room ultraviolet germicidal irradiation (UVGI) system in learning environments: effects of ventilation rate, UV fluence rate, and UV radiating volume. *Sustain. Cities Soc.* **2022**, *85*, 104048.

(10) Park, S.; Mistrick, R.; Sitzabee, W.; Rim, D. Effect of ventilation strategy on performance of upper-room ultraviolet germicidal irradiation (UVGI) system in a learning environment. *Sci. Total Environ.* **2023**, *899*, 165454.

(11) Buonanno, M.; Welch, D.; Shuryak, I.; Brenner, D. J. Far-UVC light (222 nm) efficiently and safely inactivates airborne human coronaviruses. *Sci. Rep.* **2020**, *10* (1), 10285.

(12) Hubbard, H. F.; Coleman, B. K.; Sarwar, G.; Corsi, R. L. Effects of an ozone-generating air purifier on indoor secondary particles in three residential dwellings. *Indoor Air* **2005**, *15* (6), 432−444.

(13) Kujundzic, E.; Matalkah, F.; Howard, C. J.; Hernandez, M.; Miller, S. L. UV air cleaners and upper-room air ultraviolet germicidal irradiation for controlling airborne bacteria and fungal spores. *J. Occup. Environ. Hyg.* **2006**, *3* (10), 536−546.

(14) Yu, K. P.; Lee, G. W. M.; Hsieh, C. P.; Lin, C. C. Evaluation of ozone generation and indoor organic compounds removal by air cleaners based on chamber tests. *Atmos. Environ.* **2011**, *45* (1), 35−42.

(15) Guo, C.; Gao, Z.; Shen, J. Emission rates of indoor ozone emission devices: a literature review. *Build. Environ.* **2019**, *158*, 302−318.
(16) Peng, Z.; Jimenez, J. L. Radical chemistry in oxidation flow reactors for atmospheric chemistry research. *Chem. Soc. Rev.* **2020**, *49* (9), 2570−2616.
(17) Collins, D. B.; Farmer, D. K. Unintended consequences of air cleaning chemistry. *Environ. Sci. Technol.* **2021**, *55* (18), 12172−12179.
(18) Joo, T.; Rivera-Rios, J. C.; Alvarado-Velez, D.; Westgate, S.; Ng, N. L. Formation of oxidized gases and secondary organic aerosol from a commercial oxidant-generating electronic air cleaner. *Environ. Sci. Technol. Lett.* **2021**, *8* (8), 691−698.
(19) Lee, L. D.; Delclos, G.; Berkheiser, M. L.; Barakat, M. T.; Jensen, P. A. Evaluation of multiple fixed in-room air cleaners with ultraviolet germicidal irradiation, in high-occupancy areas of selected commercial indoor environments. *J. Occup. Environ. Hyg.* **2022**, *19* (1), 67−77.
(20) Graeffe, F.; Luo, Y.; Guo, Y.; Ehn, M. Unwanted indoor air quality effects from using ultraviolet C lamps for disinfection. *Environ. Sci. Technol. Lett.* **2023**, *10* (2), 172−178.
(21) Peng, Z.; Miller, S. L.; Jimenez, J. L. Model evaluation of secondary chemistry due to disinfection of indoor air with germicidal ultraviolet lamps. *Environ. Sci. Technol. Lett.* **2023**, *10* (1), 6−13.
(22) McConnell, R.; Berhane, K.; Gilliland, F.; London, S. J.; Islam, T.; Gauderman, W. J.; Avol, E.; Margolis, H. G.; Peters, J. M. Asthma in exercising children exposed to ozone: a cohort study. *Lancet* **2002**, *359* (9304), 386−391.
(23) Ciencewicki, J.; Trivedi, S.; Kleeberger, S. R. Oxidants and the pathogenesis of lung diseases. *J. Allergy Clin. Immunol.* **2008**, *122* (3), 456−468.
(24) Pekkanen, J.; Peters, A.; Hoek, G.; Tiittanen, P.; Brunekreef, B.; de Hartog, J.; Heinrich, J.; Ibald-Mulli, A.; Kreyling, W. G.; Lanki, T.; et al. Particulate air pollution and risk of ST-segment depression during repeated submaximal exercise tests among subjects with coronary heart disease: the exposure and risk assessment for fine and ultrafine particles in ambient air (ULTRA) study. *Circulation* **2002**, *106* (8), 933−938.
(25) Won, Y.; Lakey, P. S.; Morrison, G.; Shiraiwa, M.; Rim, D. Spatial distributions of ozonolysis products from human surfaces in ventilated rooms. *Indoor Air* **2020**, *30* (6), 1229−1240.
(26) Zannoni, N.; Lakey, P. S.; Won, Y.; Shiraiwa, M.; Rim, D.; Weschler, C. J.; Wang, N.; Ernle, L.; Li, M.; Bekö, G.; et al. The human oxidation field. *Science* **2022**, *377* (6610), 1071−1077.
(27) Steinemann, A.; Nematollahi, N.; Rismanchi, B.; Goodman, N.; Kolev, S. D. Pandemic products and volatile chemical emissions. *Air Qual. Atmos. Health* **2021**, *14*, 47−53.
(28) Bruchard, W.; Bajracharya, A.; Johnston, N. A. Volatile organic compound emissions from disinfectant usage in the home and office. *Environ. Health Perspect.* **2023**, *131* (4), 047701.
(29) Kang, I.-S.; Xi, J.; Hu, H.-Y. Photolysis and photooxidation of typical gaseous VOCs by UV irradiation: removal performance and mechanisms. *Front. Environ. Sci. Eng.* **2018**, *12*, 8.
(30) Barber, V. P.; Goss, M. B.; Franco Deloya, L. J.; LeMar, L. N.; Li, Y.; Helstrom, E.; Canagaratna, M.; Keutsch, F. N.; Kroll, J. H. Indoor air quality implications of germicidal 222 nm light. *Environ. Sci. Technol.* **2023**, *57* (42), 15990−15998.
(31) Link, M. F.; Shore, A.; Hamadani, B. H.; Poppendieck, D. Ozone generation from a germicidal ultraviolet lamp with peak emission at 222 nm. *Environ. Sci. Technol. Lett.* **2023**, *10* (8), 675−679.
(32) Peng, Z.; Day, D. A.; Symonds, G. A.; Jenks, O. J.; Stark, H.; Handschy, A. V.; de Gouw, J. A.; Jimenez, J. L. Significant production of ozone from germicidal UV lights at 222 nm. *Environ. Sci. Technol. Lett.* **2023**, *10* (8), 668−674.
(33) ANSI/ASHRAE. *Standard 62.1−2019: Ventilation for Acceptable Indoor Air Quality*; ASHRAE, 2019.
(34) Rim, D.; Novoselac, A. Ventilation effectiveness as an indicator of occupant exposure to particles from indoor sources. *Build. Environ.* **2010**, *45* (5), 1214−1224.
(35) ASHRAE. *Fundamentals, Chapter 18: Nonresidential Cooling and Heating Load Calculations*; ASHRAE: Atlanta, GA, USA, 2021.
(36) Shan, W.; Rim, D. Thermal and ventilation performance of combined passive chilled beam and displacement ventilation systems. *Energy Build.* **2018**, *158*, 466−475.
(37) Gupta, J. K.; Lin, C. H.; Chen, Q. Characterizing exhaled airflow from breathing and talking. *Indoor Air* **2010**, *20* (1), 31−39.
(38) Ai, Z. T.; Melikov, A. K. Airborne spread of expiratory droplet nuclei between the occupants of indoor environments: a review. *Indoor Air* **2018**, *28* (4), 500−524.
(39) Menter, F. R. Two-equation eddy-viscosity turbulence models for engineering applications. *AIAA J.* **1994**, *32* (8), 1598−1605.
(40) Pei, G.; Rim, D. Quality control of computational fluid dynamics (CFD) model of ozone reaction with human surface: effects of mesh size and turbulence model. *Build. Environ.* **2021**, *189*, 107513.
(41) Langer, S.; Moldanová, J.; Arrhenius, K.; Ljungström, E.; Ekberg, L. Ultrafine particles produced by ozone/limonene reactions in indoor air under low/closed ventilation conditions. *Atmos. Environ.* **2008**, *42* (18), 4149−4159.
(42) Khamaganov, V. G.; Hites, R. A. Rate constants for the gas-phase reactions of ozone with isoprene, α- and β-pinene, and limonene as a function of temperature. *J. Phys. Chem. A* **2001**, *105* (5), 815−822.
(43) Calvert, J. G. *Mechanisms of Atmospheric Oxidation of the Alkanes*; Oxford University Press, 2008.
(44) Atkinson, R.; Baulch, D. L.; Cox, R. A.; Crowley, J. N.; Hampson, R. F.; Hynes, R. G.; Jenkin, M. E.; Rossi, M. J.; Troe, J. Evaluated kinetic and photochemical data for atmospheric chemistry: volume I-gas phase reactions of O_x, HO_x, NO_x and SO_x species. *Atmos. Chem. Phys.* **2004**, *4* (6), 1461−1738.
(45) Mollner, A. K.; Valluvadasan, S.; Feng, L.; Sprague, M. K.; Okumura, M.; Milligan, D. B.; Bloss, W. J.; Sander, S. P.; Martien, P. T.; Harley, R. A.; et al. Rate of gas phase association of hydroxyl radical and nitrogen dioxide. *Science* **2010**, *330* (6004), 646−649.
(46) Hofzumahaus, A.; Stuhl, F. Rate constant of the reaction HO + CO in the presence of N_2 and O_2. *Ber. Bunsenges. Phys. Chem.* **1984**, *88* (6), 557−561.
(47) Won, Y.; Waring, M.; Rim, D. Understanding the spatial heterogeneity of indoor OH and HO_2 due to photolysis of HONO using computational fluid dynamics simulation. *Environ. Sci. Technol.* **2019**, *53* (24), 14470−14478.
(48) Weschler, C. J. Ozone's impact on public health: contributions from indoor exposures to ozone and products of ozone-initiated chemistry. *Environ. Health Perspect.* **2006**, *114* (10), 1489−1496.
(49) Niu, Y.; Cai, J.; Xia, Y.; Yu, H.; Chen, R.; Lin, Z.; Liu, C.; Chen, C.; Wang, W.; Peng, L.; et al. Estimation of personal ozone exposure using ambient concentrations and influencing factors. *Environ. Int.* **2018**, *117*, 237−242.
(50) Salonen, H.; Salthammer, T.; Morawska, L. Human exposure to ozone in school and office indoor environments. *Environ. Int.* **2018**, *119*, 503−514.
(51) Lee, K.; Vallarino, J.; Dumyahn, T.; Ozkaynak, H.; Spengler, J. D. Ozone decay rates in residences. *J. Air Waste Manag. Assoc.* **1999**, *49* (10), 1238−1244.
(52) Holøs, S. B.; Yang, A.; Lind, M.; Thunshelle, K.; Schild, P.; Mysen, M. VOC emission rates in newly built and renovated buildings, and the influence of ventilation—a review and meta-analysis. *Int. J. Vent.* **2019**, *18* (3), 153−166.
(53) Wang, N.; Ernle, L.; Beko, G.; Wargocki, P.; Williams, J. Emission rates of volatile organic compounds from humans. *Environ. Sci. Technol.* **2022**, *56* (8), 4838−4848.
(54) Yeoman, A. M.; Shaw, M.; Carslaw, N.; Murrells, T.; Passant, N.; Lewis, A. C. Simplified speciation and atmospheric volatile organic compound emission rates from non-aerosol personal care products. *Indoor Air* **2020**, *30* (3), 459−472.

https://doi.org/10.1021/acs.est.4c00575
Environ. Sci. Technol. 2024, 58, 12051−12061

(55) Dlugokencky, E.; Houweling, S. Chemistry of the atmosphere: methane. In *Encyclopedia of Atmospheric Sciences*, 2nd ed.; Elsevier Inc., 2015..
(56) Sander, S. P.; Abbatt, J.; Barker, J. R.; Burkholder, J. B.; Friedl, R. R.; Golden, D. M.; Wine, P. H. *Chemical Kinetics and Photochemical Data for Use in Atmospheric Studies*. Evaluation No. 17; JPL Publication, 2006. http://jpldataeval.jpl.nasa.gov/.
(57) Whalen, J. *Environmental Control for Tuberculosis: Basic Upper Room Ultraviolet Germicidal Irradiation Guidelines for Health Care Settings*; National Institutes of Occupational Safety and Health: Cincinnati, OH. Report No. DHHS (NIOSH). Publication No. 2009-015, 2009. https://stacks.cdc.gov/view/cdc/5306.
(58) Kalliomäki, P.; Sobhani, H.; Stratton, P.; Coleman, K. K.; Srikakulapu, A. K.; Salawitch, R. J.; Dickerson, R. R.; Zhu, S.; Srebric, J.; Milton, D. K. Ozone and ultra-fine particle concentrations in a hotel quarantine facility during 222 nm far-UVC air disinfection. *medRxiv* **2023**, 2023-09.
(59) Liu, S.; Koupriyanov, M.; Paskaruk, D.; Fediuk, G.; Chen, Q. Investigation of airborne particle exposure in an office with mixing and displacement ventilation. *Sustain. Cities Soc.* **2022**, *79*, 103718.
(60) Park, S.; Lee, S.; Yeo, M. S.; Rim, D. Performance of a heat recovery ventilation system for controlling human exposure to airborne particles in a residential building. *Build. Environ.* **2023**, *239*, 110412.
(61) Nazaroff, W. W.; Weschler, C. J. Indoor ozone: concentrations and influencing factors. *Indoor Air* **2022**, *32* (1), No. e12942.
(62) Lakey, P. S.; Won, Y.; Shaw, D.; Østerstrøm, F. F.; Reidy, E.; Shiraiwa, M. Spatial and temporal scales of variability for indoor air constituents. *Communications Chemistry* **2021**, *4* (1), 110.
(63) The Lancet COVID-19 commission. *Proposed Non-Infectious Air Deliver Rates (NADR) for Reducing Exposure to Airborne Respiratory Infectious Diseases*, 2022. https://covid19commission.org/safe-work-travel.
(64) Gligorovski, S.; Strekowski, R.; Barbati, S.; Vione, D. Environmental implications of hydroxyl radicals (•OH). *Chem. Rev.* **2015**, *115* (24), 13051−13092.
(65) Lin, Z.; Chow, T. T.; Fong, K. F.; Tsang, C. F.; Wang, Q. Comparison of performances of displacement and mixing ventilations. Part II: indoor air quality. *Int. J. Refrig.* **2005**, *28* (2), 288−305.
(66) Deevy, M.; Sinai, Y.; Everitt, P.; Voigt, L.; Gobeau, N. Modelling the effect of an occupant on displacement ventilation with computational fluid dynamics. *Energy Build.* **2008**, *40* (3), 255−264.
(67) Choi, E.; Tan, Z.; Anderson, W. A. Formation of secondary organic aerosols by germicidal ultraviolet light. *Environments* **2019**, *6* (2), 17.
(68) Stockwell, W. R. Effects of turbulence on gas-phase atmospheric chemistry: calculation of the relationship between time scales for diffusion and chemical reaction. *Meteorol. Atmos. Phys.* **1995**, *57* (1−4), 159−171.
(69) Elperin, T.; Kleeorin, N.; Rogachevskii, I. Effect of chemical reactions and phase transitions on turbulent transport of particles and gases. *Phys. Rev. Lett.* **1998**, *80* (1), 69−72.
(70) Beggs, C. B.; Sleigh, P. A. A quantitative method for evaluating the germicidal effect of upper room UV fields. *J. Aerosol Sci.* **2002**, *33* (12), 1681−1699.
(71) Rim, D.; Gall, E. T.; Kim, J. B.; Bae, G. N. Particulate matter in urban nursery schools: a case study of Seoul, Korea during winter months. *Build. Environ.* **2017**, *119*, 1−10.
(72) Kim, J.; Park, S.; Kim, H.; Yeo, M. S. Emission characterization of size-resolved particles in a pre-school classroom in relation to children's activities. *Indoor Built Environ.* **2019**, *28* (5), 659−676.
(73) Rossignol, S.; Rio, C.; Ustache, A.; Fable, S.; Nicolle, J.; Même, A.; D'Anna, B.; Nicolas, M.; Leoz, E.; Chiappini, L. The use of a housecleaning product in an indoor environment leading to oxygenated polar compounds and SOA formation: gas and particulate phase chemical characterization. *Atmos. Environ.* **2013**, *75*, 196−205.
(74) Kang, D. H.; Choi, D. H.; Lee, S. M.; Yeo, M. S.; Kim, K. W. Effect of bake-out on reducing VOC emissions and concentrations in a residential housing unit with a radiant floor heating system. *Build. Environ.* **2010**, *45* (8), 1816−1825.
(75) Cummings, B. E.; Li, Y.; DeCarlo, P. F.; Shiraiwa, M.; Waring, M. S. Indoor aerosol water content and phase state in US residences: impacts of relative humidity, aerosol mass and composition, and mechanical system operation. *Environ. Sci.: Process. Impacts* **2020**, *22* (10), 2031−2057.
(76) Lim, A. Y.; Yoon, M.; Kim, E. H.; Kim, H. A.; Lee, M. J.; Cheong, H. K. Effects of mechanical ventilation on indoor air quality and occupant health status in energy-efficient homes: a longitudinal field study. *Sci. Total Environ.* **2021**, *785*, 147324.

https://doi.org/10.1021/acs.est.4c00575
Environ. Sci. Technol. 2024, 58, 12051−12061